Journal of Materials Chemistry A

PAPER

View Article Online
View Journal | View Issue

Cite this: J. Mater. Chem. A, 2015, 3, 13357

Carbon dots modified mesoporous organosilica as an adsorbent for the removal of 2,4-dichlorophenol and heavy metal ions†

Lingzhi Wang,[ab] Chen Cheng,[a] Sen Tapas,[c] Juying Lei,[a] Masaya Matsuoka,[d] Jinlong Zhang*[a] and Fan Zhang*[b]

Received 4th March 2015
Accepted 14th May 2015

DOI: 10.1039/c5ta01652e

www.rsc.org/MaterialsA

Periodic mesoporous organosilica embedded with carbon dots are adopted as the adsorbent for removal of the toxic organic pollutant 2,4-dichlorophenol and inorganic metal ions Hg(II), Cu(II), and Pb(II). The composite possesses an ordered 2D hexagonal mesostructure with a space group of *p6mm*, high specific surface area (~468.46 m^2 g^{-1}), and uniform pore size (~5.50 nm). The surface is covered by about 1–2 layers of carbon dot nanoparticles. The maximum adsorption capacity for 2,4-dichlorophenol is 99.70 mg g^{-1}, and the distribution coefficient of metal ions between adsorbent and solution phases is in the range of 2.60–7.41, following the order of Hg(II) > Cu(II) > Pb(II). The Cu(II) and Pb(II) adsorption stays nearly fixed while Hg(II) adsorption is depressed by ~45% in a mixed solution of metal ions. The Cu(II) and Hg(II) adsorption shows unapparent variation but Pb(II) adsorption is improved by ~55% in a mixed solution of metal ion and 2,4-dichlorophenol. In contrast, all metal ions lead to the depression of 2,4-dichlorophenol adsorption by 37% (Pb(II)), 45% (Cu(II)), and 48% (Hg(II)). Finally, the n–π electron donor–acceptor interaction between O- and N-containing groups in mesoporous organosilica and the benzene ring in 2,4-dichlorophenol is revealed to be responsible for the enhanced adsorption of 2,4-dichlorophenol, while the electrostatic force and complex formation between metal ions and amide groups co-contribute to the improvement of metal ions adsorption.

Introduction

Mesoporous silica is a group of materials with large specific surface areas, long-range ordered pore channels, and highly tunable pore sizes. Since the first invention in 1992,[1] they have been widely applied for pollutants removal.[2–5] However, the adsorption behavior of pollutants on pristine mesoporous silica is comparatively simple, mainly depending on electrostatic or hydrogen interactions with silanol groups.[6] In consideration of the complexity of pollutants in the real environment, many efforts have been devoted to tailor mesoporous characteristics (space group symmetry, pore size, surface area, *etc.*) and surface chemistry.[7–9] Removal of versatile pollutants from sewage has been achieved and was helped by many diverse ways available for tuning characteristics, which complement an existing suite of relatively unspecific conventional sorbents.[10–14]

Besides diverse tunable properties, the eventual application of mesoporous silica for real sewage treatment poses complicated requirements for adding adsorbents from synthesis, functionalization processes, and pore ordering. Developing a cheap and convenient way to fabricate multiple-group functionalized mesoporous silica adsorbents, with an ordered pore channel system, is desirable in order to meet demands for pollutant removal; however, this still remains a great challenge. Moreover, current research has mainly focused on isolated sorptions of single metal ions or organic contaminants with mesoporous silica and ignored any potential interactions between metal ions and organic contaminants that may influence sorption. A single-solute system may not adequately represent the majority of mixed contaminants commonly encountered in the environment, where complex mixtures of pollutants containing both heavy metals and organic contaminants may coexist at many sites. To the best of our knowledge, the question as to whether metals affect the sorption of organic contaminants and *vice versa* on mesoporous silica has not been adequately addressed.[15–17] The reason for lack of a comprehensive study about pollutant removal actually lies with problems of introducing versatile functional groups on mesoporous

[a]Key Lab for Advanced Materials, Institute of Fine Chemicals, East China University of Science and Technology, Shanghai, 200237, P. R. China. E-mail: jlzhang@ecust.edu.cn
[b]Department of Chemistry and Laboratory of Advanced Materials, iChEm (Collaborative Innovation Center for Energy Materials), State Key Laboratory of Molecular Engineering of Polymers, Fudan University, Shanghai 200433, P. R. China. E-mail: zhang_fan@fudan.edu.cn
[c]Centre for Materials Science, Institute of Nanotechnology and Bioengineering, School of Forensic and Investigative Sciences, University of Central Lancashire, Preston, UK
[d]Department of Applied Chemistry, Graduate School of Engineering, Osaka Prefecture University, Osaka 599-8531, Japan

† Electronic supplementary information (ESI) available. See DOI: 10.1039/c5ta01652e

silica without sacrificing pore accessibility using simple synthesis procedures.

In this study, 2D hexagonal mesoporous silica with a space group of *p6mm* was synthesized using triblock copolymer P123 as the template through the co-condensation of silylated carbon dots (CD)[18,19] and tetraethylorthosilicate (TEOS). CD was chosen since it is a triethoxysilane that assembles functional groups of amide and aromatic rings. It is prepared through a fast and convenient pyrolysis process of citric acid and amine-containing silane. This hybrid material possesses specific surface area of 468.46 $m^2\ g^{-1}$, pore size of 5.50 nm and pore volume of 0.76 $cm^3\ g^{-1}$. Besides silanols, the surface is covered with multiple groups of amides and aromatic rings, and the atom weights of C and N are 18.3% and 2.7%, respectively. We applied this multi-modified mesoporous silica to the removal of organic 2,4-dichlorophenol (2,4-DCP) and inorganic heavy metals including Cu(II), Pb(II) and Hg(II). 2,4-DCP was chosen as a model for organic pollutants because chlorophenol derivatives play vital roles as intermediates for the synthesis of dyes and pesticides and also it is hard to biodegrade. Moreover, the commonly adopted chlorination disinfection process for sewage water further deteriorates the pollution situation caused by chlorophenol derivatives. Heavy metals Cu(II), Pb(II) and Hg(II) commonly exist in the soil environment, especially in soil irrigated by wastewater in countries with water shortages. Previous work was reported with the sorption of metal ions and chlorophenol on mesoporous silica separately,[20–25] whereas in this paper we focus on the competitive adsorption between metal ions, the effect of metal ions on 2,4-DCP sorption and *vice versa*, and on the relevant mechanisms in particular.

Experimental

Synthesis of CD

Silylated CD nanoparticles were obtained by a one-step high-temperature pyrolysis method described previously.[19] First, 10 mL of *N*-(β-aminoethyl)-γ-aminopropyl methyldimethoxy silane (AEAPMS) was heated to 240 °C under magnetic stirring and nitrogen atmosphere. Then, 0.5 g of anhydrous citric acid was quickly added into the flask. The mixture was heated for 1 min, and was then gradually cooled down to room temperature. The CD NPs were obtained by washing the crude product twice with hexane, sealed with hexane, and stored in a refrigerator for further use.

Synthesis of CD modified mesoporous organosilica

CD modified mesoporous silica was prepared by using triblock copolymer Pluronic P123 ($EO_{20}PO_{70}EO_{20}$, $M_{av} = 5800$, Aldrich) as the template, and silylated CD and TEOS as the silica co-precursor.[28] Typically, 4.0 g of Pluronic P123 was dissolved in 120 mL of HCl solution (2.0 M) to get a homogeneous solution by vigorous stirring at 38 °C. Then, 9 mL of TEOS and an appropriate amount of as-made CD was dropwise added and stirred continually at 38 °C for 24 h. Then the mixture was transferred to an autoclave and hydrothermally treated at 100 °C for 24 h. The as-made sample was filtered, washed with deionized water, and dried at 60 °C under vacuum. To remove the surfactant, 50 mg of the as-made samples and 60 mg of sodium acetate were added into 5 mL of ethanol. The mixture was then stirred under reflux at 92 °C for 1 h, washed and dried. The final product was named as CD-MS.

Batch adsorption

Organic 2,4-DCP and inorganic Cu(II), Pb(II) and Hg(II) ions were adopted as pollutant models. The solution pH was adjusted with 0.1 M of HNO_3. Adsorption kinetic and thermodynamic experiments were carried out to investigate adsorption equilibrium times, confirm adsorption types, and assess adsorption rates. For the study on isolate adsorption, 60 mg L^{-1} of 2,4-DCP, 10^{-3} M of Cu $(NO_3)_2$, Pb $(NO_3)_2$ and Hg $(NO_3)_2$ were prepared and used as a stock solution unless otherwise noted. Adsorbent doses for the isolate adsorptions of metal ions and 2,4-DCP were 1.0 and 0.2 g L^{-1}, respectively. A mixture was put into a gas bath thermostatic oscillator, and shaken at a certain temperature for 3 h. Then the mixture was centrifuged at 12 000 rpm for 10 min. The obtained liquid was filtered through syringe filters (cellulose acetate membranes) with a size of 0.22 μm to remove particles after the adsorption, and diluted 10 times for characterization by inductively coupled plasma-atomic emission spectroscopy (ICP-AES) or UV-Vis spectroscopy. The adsorption competitions between metal ions and 2,4-DCP, and different metal ions were investigated in the presence of 1.0 g L^{-1} adsorbent. For mixed metal ions and mixed metal ion–2,4-DCP solutions, the respective concentration of each component remained the same as that in the isolate solution unless otherwise noted. For the reusability analysis, absolute ethyl alcohol and acidic solutions were used for the desorption of 2,4-DCP and metal ions.[26,27] The adsorbent was first centrifuged after the adsorption process, then dispersed in ethyl alcohol or HNO_3 water solution with a pH value of 1.0 ± 0.1 to form a solution containing 1 g L^{-1} of adsorbent. The adsorbent was centrifuged from the mixture after being shaken in a gas bath thermostatic oscillator for 3 h, repeatedly washed by deionized water to ensure the complete removal of adsorbate, dried, and used for the next sorption cycle.

Characterization

X-ray diffraction (XRD) patterns were collected in the range of 0.5–5° (2θ) on a RigakuD/MAX 2550 diffractometer using Cu Kα radiation (40 kV, 100 mA, $\lambda = 0.15406$ nm). N_2 sorption isotherms were measured at 77 K by a Micromeritics ASAP 2020 analyzer. The Brunauer–Emmett–Teller (BET) method was utilized to calculate specific surface areas (SBET) by using the Barrett–Joyner–Halenda (BJH) model; pore volumes and pore size distributions were derived from the adsorption branches of isotherms. Transmission electron microscopy (TEM) was conducted on a JEM 2000EX microscope. ^{1}H 2D Diffusion-Ordered Spectroscopy-Nuclear Magnetic Resonance (DOSY-NMR) spectrum was performed on a Bruker AM 400 MHz NMR spectrometer. The width of the gradient pulse was 1 ms, and the diffusion time was 150 ms. Fourier Transform Infrared (FT-IR) spectra were recorded with a Nicolet FTIR spectrometer (Nicolet

Magna 550). UV-Vis absorption or diffuse reflection spectra were performed on a Scan UV-Vis spectrophotometer (SHIMADZU, UV-2450), with $BaSO_4$ as the reflectance sample. Zeta-potential *vs.* pH curves were analyzed by a Malvern Zetasizer Nano-ZS instrument (ZEN3600, Malvern Instruments), using 0.1 M of NaOH and HCl to adjust the pH value, and 0.1 M of NaCl to maintain a high background-electrolyte concentration. The energy dispersive X-ray (EDX) spectrum was performed on an EDAX instrument. High performance liquid chromatography (HPLC, SHIMADZU LC-20A) was used to test the concentration of 2,4-DCP (flow rate: 1 mL per min, mobile phase: 60% acetonitrile, column temperature: 40 °C, determinate wavelength: 282 nm). Water repellency was determined by a contact angle analysis using a contact angle meter (Dataphysic OCA20). The photoluminescence emission spectrum was obtained from a fluorescence spectrophotometer (SHIMADZU RF5301-PC). Concentrations of metal ions were measured using an inductively coupled plasma-atomic emissions spectrometer (ICP-AES, Vanan 710). The peak positions of Cu(II), Pb(II) and Hg(II) were 327, 220 and 253, respectively.

Results

Structure analyses

CD modified mesoporous silica (CD-MS) was synthesized through the self-assembly of silylated CD, TEOS, and triblock copolymer P123 template. The template was removed by refluxing the as-made sample in a sodium acetate EtOH solution. The small-angle XRD pattern of CD-MS after template-extraction showed three finely-resolved peaks at $2\theta = 0.92$, 1.62 and 1.86° (Fig. 1a), ascribing to the 100, 110 and 200 reflections of a 2D hexagonal mesostructure with a space group of *p6mm*.[29] The unit-cell parameter (a_0) was calculated to be 11.76 nm. The transmission electronic microscopy (TEM) image verifies that CD-MS possesses a highly ordered parallel-aligned pore channel system (Fig. S1†).

The N_2 sorption isotherms (Fig. 1b) show typical type IV curves with sharp capillary condensation steps and a H1 hysteresis loop in the middle P/P_0 range of 0.5–0.8; these are characteristics of an ordered mesoporous structure and coincident with the results from XRD patterns and the TEM image. The specific surface area was calculated to be ~468.46 $m^2\ g^{-1}$ by the Brunauer–Emmett–Teller (BET) method (Table 1). A narrow pore-size distribution curve with the mean value of ~5.50 nm was obtained from the adsorption branch using the Barrett–Joyner–Halenda (BJH) model. The pore volume is about 0.76 $cm^3\ g^{-1}$. In comparison, the pristine mesoporous silica prepared using TEOS as the single source, and through the template-extraction method (MS-ex), has a comparable value of a_0 (10.19 nm) but increased pore size (7.78 nm), which becomes even larger (9.88 nm) when the template is removed by calcination (MS-cal). The particle size of CDs was determined as ~1.0 nm by the ^1H 2D DOSY-NMR spectrum (Fig. S2†). Incorporation of CDs causes a 2.89 nm increase of wall thickness and a 2.28 nm decrease of pore size according to the estimated wall thicknesses of CD-MS (5.30 nm) and pristine mesoporous silica MS-ex (2.41 nm) on the basis of the hexagonal pore structure, suggesting that the pore surface is covered by 1–2 layers of CD NPs.

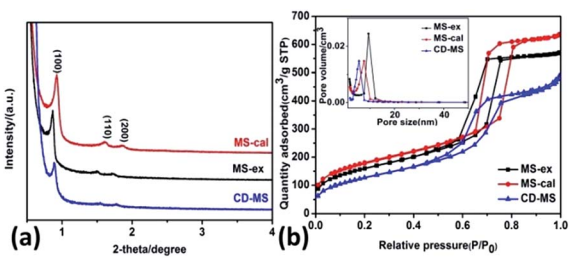

Fig. 1 Small-angle XRD patterns (a) and N_2 sorption isotherms (b) of MS-cal, MS-ex and CD-MS. Inset is the pore size distribution.

FT-IR spectra (Fig. 2a) of CD-MS show bands at ~3400, 1650, 1450 cm^{-1}, 1100 and 960 cm^{-1}. The bands at 3400 cm^{-1} can be assigned to –OH stretching from the silanol groups. Presence of the $CONH_2$ group is verified by the bands at 1650 and 1450 cm^{-1}.[17] The bands at 1100 and 960 cm^{-1} are ascribed to characteristic Si–O–Si and Si–OH vibrations.[30] Moreover, CD-MS shows an absorption band with the maximum absorption wavelength at ~400 nm (Fig. 2b) and a strong fluorescence emission centred at ~520 nm (inset, Fig. 2b), which should result from the conjugated aromatic ring in CD. Compared with the emission from CD, the widened emission spectrum of CD-MS is caused by the heterogeneous state of CD in solid mesoporous silica. The EDX spectrum further proves CD-MS contains about 18.3 at% of C, 2.7 at% of N, 33.1 at% of Si and 45.9 at% of O (at = atom percentage, Fig. 2d). The isoelectric point is increased from pH = 2 to 5 due to the embedding of CD NP (Fig. 2c), ascribed to the presence of an amide group in CD.[6]

Adsorption of 2,4-DCP

2,4-DCP was adopted as a model for organic pollutants due to the high toxicity and difficult biodegradability of chlorophenol derivatives.[21] As shown in Fig. 3a, CD-MS shows ~30% capture percentage for 2,4-DCP with an initial concentration of 60 mg L^{-1} at 10 °C, corresponding to a high equilibrium adsorption capacity (q_e) of 96.10 mg g^{-1}. The adsorption is much more efficient than that on MS-ex (~6.8%, $q_e = 16.5$ mg g^{-1}) and MS-cal (2.5%, $q_e = 7.5$ mg g^{-1}). The surfactant in as-made CD-MS was removed through a solvent-extraction procedure, suggesting that the silanol groups are partly responsible for the improved adsorption. Moreover, the capture percentage prominently decreases with increasing pH values of the solution from 2–8, (Fig. 3b), indicative of the negative effect of protonation (sorbate and sorbent) on adsorption behavior.[31] The adsorption thermodynamic data of 2,4-DCP on CD-MS (Fig. 3c) are simulated by Langmuir and the logarithmic form of Freundlich models, respectively (Fig. S3†), indicating that the Langmuir model is more suitable to describe the adsorption behavior with the linear coefficient R^2 value close to 1 (Tables 2 and S1†). In the Langmuir model, it is assumed that all the adsorption sites of the adsorbent have an identical binding energy and each of them binds to only a single layer of adsorbate molecules.[32] In

Table 1 Structural and textural parameters of CD-MS, MS-ex and MS-cal

Samples	S_{BET} (m^2 g^{-1})	V_{pore} (cm^3 g^{-1})	d_{pore} (nm)	a_0 (nm)	d (nm)	d_{wall} (nm)
CD-MS	468.46	0.76	5.50	11.76	10.17	5.30
MS-ex	584.87	0.88	7.78	10.19	8.83	2.41
MS-cal	598.65	0.93	9.88	11.40	9.87	1.52

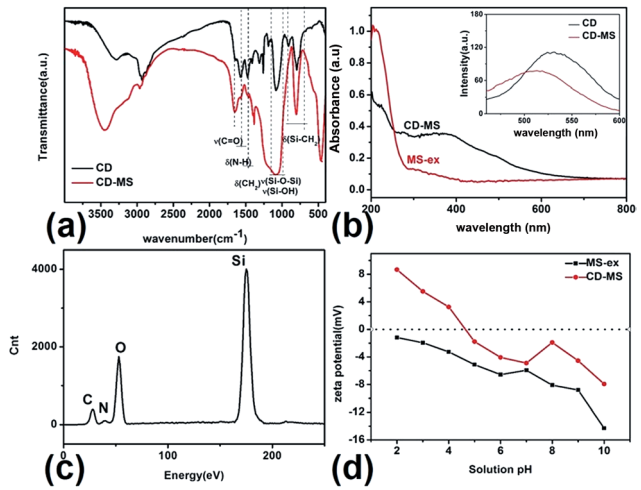

Fig. 2 FT-IR spectra of CD and CD-MS (a); diffuse reflection UV-vis spectra of MS-ex and CD-MS (b), inset is the fluorescence emission spectra of CD and CD-MS; EDX spectrum of CD-MS (c); relation between zeta potential and solution pH of MS-ex and CD-MS (d).

addition, the maximum adsorption amount of 2,4-DCP increases from 96.81 to 105.5 mg g^{-1} with increasing temperature from 10 to 35 °C (Fig. 3c, S4,† and Table 2), revealing the occurrence of an endothermic adsorption process.[4] Data about adsorption kinetics of 2,4-DCP on CD-MS (Fig. 3d) were simulated using pseudo-first-order and pseudo-second-order kinetic models, revealing it is more accordant with a pseudo-second-order kinetic model with adsorption equilibrium values close to the measured q_e (Fig. S5 and Table S2†).[33] The recycling study showed less than 10% decrease of the adsorption capacity after 4 cycles (Fig. S6†), demonstrating the excellent reusability of CD-MS.

Adsorption of metal ions

Cu(II), Pb(II), and Hg(II) were adopted as models of heavy metal ions. CD-MS shows the capture percentages of ~53, 43 and 56% to Cu(II), Pb(II) and Hg(II) with an initial concentration of 10^{-3} M (Fig. 4a). In comparison, the same kind of pristine mesoporous silica shows similar adsorption capacity to different metal ions, but MS-ex presents higher adsorption efficiency (~40%) than MS-cal (~27%), indicating the positive effect of silanol groups on the capture of metal ions. The further improved capture ability of CD-MS to metal ions, especially for Hg(II), should be definitely related to the embedding of CD NPs. Metal ion adsorption on CD-MS is negligible at pH = 1, then reaches to a maximum at pH = 4, and finally keeps fixing in the pH range of 4–7 (Fig. 4b). The depressed adsorption in acidic solutions should be attributed to the protonation of the nitrogenous and siliceous surface of CD-MS with an isoelectric point of 5. Simulations of thermodynamic adsorption data collected at 25 °C and 35 °C (Fig. 4c) by Langmuir and logarithmic forms of Freundlich models suggest the Freundlich is more reliable than the Langmuir model based on the larger correlation factor (0.999), and imply the existence of a reversible heterogeneous adsorption and heterogeneity of binding energies at adsorption sites (Fig. S7 and Table S3†). This may result from different adsorption sites with different metal-binding energies. In addition, all the Freundlich adsorption intensity variables (n values) are >1, follow the order of Hg(II) > Cu(II) > Pb(II) (Table 3). In general, an isotherm with $n > 1$, known as L-type, indicates a strong adsorbent affinity for the adsorbate, suggesting Hg(II) and Pb(II) have the highest and least affinities to CD-MS. The higher K_f value of Hg(II) adsorption further proves a stronger adsorption force due to higher affinity between the amide groups CD-MS and Hg(II). All the n values for three kinds of metal ions decreased with increasing temperature (Fig. 4c, S8 and Table S4†), revealing an exothermic chemi-adsorption process. Similar to that for 2,4-DCP, the adsorption process for metal ions is also accordant with pseudo-second-order kinetics

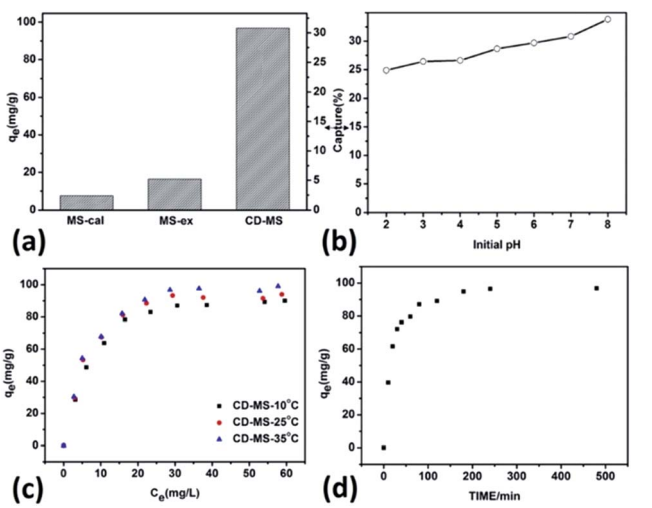

Fig. 3 Equilibrium adsorption capacity and capture percentages of 2,4-DCP on MS-cal, MS-ex and CD-MS (a); effect of solution pH on 2,4-DCP adsorption on CD-MS (b); adsorption isotherms of 2,4-DCP on CD-MS at 10, 25 and 35 °C (c); adsorption kinetic curves of 2,4-DCP on CD-MS (d). Adsorbent dose: 0.2 g L^{-1}, contact time: 3 h. (a), (b) and (d) Temperature: 10 °C, initial concentration of 2,4-DCP: 60 mg L^{-1}, pH = 7.0.

Table 2 Thermodynamic constants for the adsorption performance of 2,4-DCP at different temperatures

	Langmuir model		
Samples	q_m (mg g^{-1})	b (L mg^{-1})	R^2
MS-ex (10)	16.04	0.22	0.991
CD-MS (10)	96.81	0.23	0.991
CD-MS (25)	99.70	0.27	0.992
CD-MS (35)	105.48	0.25	0.992

Table 3 Freundlich isotherm constants and pseudo-second-order kinetics parameters for metal ions adsorptions on CD-MS[a]

	Freundlich curve			Pseudo-second-order model		
Adsorbate	K_f	n	R^2	q_{e2}	k_2	R^2
Cu(II)	3.23	1.53	0.997	68.96	2.89×10^{-3}	0.999
Pb(II)	2.60	1.38	0.993	102.35	3.40×10^{-3}	0.999
Hg(II)	7.41	1.55	0.974	132.98	1.78×10^{-3}	0.999

[a] K_f (mg$^{1-(1/n)}$L$^{1/n}$g^{-1}) is the Freundlich constant about the adsorption capacity of the adsorbents; q_{e2} (mg g^{-1}) is the adsorption capacity at adsorption equilibrium obtained through experiments; k_2 (g (mg min)$^{-1}$) is the kinetic rate constants for the pseudo-second-order models.

($R^2 \sim 1$) (Fig. 4d, S9,† and Tables 3, S3†), implying that chemical bonding might be the rate-limiting step.[34,35] Moreover, the adsorption capacity for all metal ions was shown to be well preserved after 4 recycles with negligible variation (Fig. S10†).

Competitive adsorption

Currently, there are few studies on the competition adsorption of different metal ions, and the influence of metal ions on the sorption of organics, and conversely organics, to metal adsorption on mesoporous silica adsorbents. Here, CD-MS was further adopted as the adsorbent for treatment of a multi-component polluted solution. In a mixed Cu(II)–Pb(II)–Hg(II) system, all three metal ions displayed adsorption behavior that was well fitted to the Freundlich model (Fig. 5a, Table 4), proving that the mixed system did not influence heterogeneous adsorption behavior of the respective metal ions. However, compared with the adsorption capacity in an isolated component solution, Hg(II) adsorption suffered ~45% decrease while Cu(II) and Pb(II) adsorption showed negligible variation (Fig. 5b) in the mixed solution. The concentrations of respective metal ions in mixed solutions were the same as in isolate solutions, leading to an increase of total metal ion concentrations. The preserved adsorption capacity for Cu(II) and Pb(II) at least indicates that the mesoporous adsorbent has enough volume to accommodate a large amount of metal ions. The reason for the decrease of Hg(II) adsorption will be analysed in the following discussion section.

In a mixed organics–inorganics system (Fig. 5c and d), the presence of 2,4-DCP (60 mg L^{-1}) does not change the adsorption mode of metal ions, which can still be well fitted by the Freundlich model. However, study of the adsorption capacity indicates that the presence of 2,4-DCP leads to about 45% increase of Pb(II) adsorption in the initial concentration range of 0–80 mg L^{-1}. Cu(II) and Hg(II) adsorptions present less than 10% increase and decrease, respectively. The variation of adsorption capacity with metal ions indicates that a

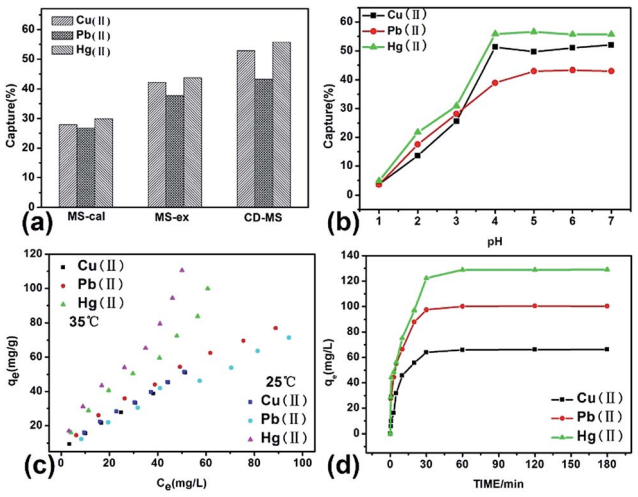

Fig. 4 Capture percentages of Cu(II), Pb(II) and Hg(II) on MS-cal, MS-ex and CD-MS (a); effect of pH on metal ion adsorption on CD-MS (b); adsorption isotherms of different metal ions on CD-MS at 25 and 35 °C (c); adsorption kinetic curves of metal ions on CD-MS (d). Adsorbent dose: 1 g L^{-1}, contact time: 3 h. Initial concentration of Hg(II) and Pb(II): 10^{-3} M, (a) and (b) initial Cu(II) concentration: 10^{-3} M, (c) and (d) initial Cu(II) concentration 2×10^{-3} M. (a), (b) and (d) Temperature: 25 °C, pH = 7.0.

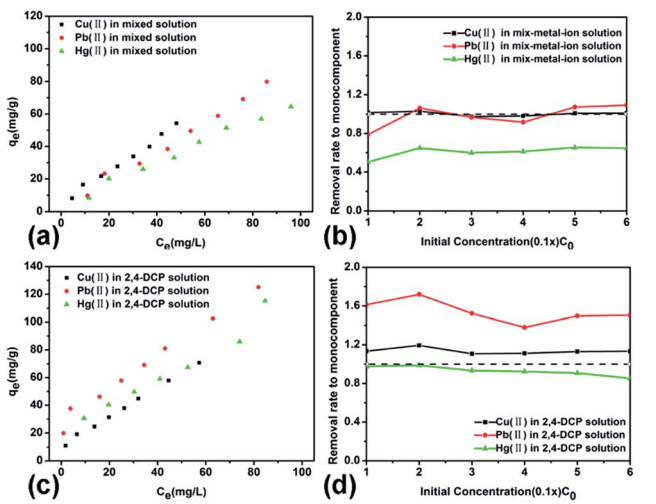

Fig. 5 Adsorption competitions in tri-metal ion and metal ion–2,4-DCP solutions (a); removal rate of metal ion in tri-metal ion system to mono-component solution (b); metal ion adsorption in the mixed solution of metal ion–2,4-DCP (c); removal rate of metal ions in metal ion–2,4-DCP mixed solution to mono-metal solution (d). Adsorbent dose: 1 g L^{-1}, contact time: 3 h, temperature: 25 °C, concentration of 2,4-DCP: 60 mg L^{-1}.

Table 4 Freundlich constants of metal ion adsorption on CD-MS in tri-metal ion solution and metal ion–2,4-DCP solution

	Freundlich model parameters					
	Triple-metal ion solution			Metal ion–2,4-DCP solution		
Adsorbate	K_f	n	R^2	K_f	n	R^2
Cu(II)	2.68	1.32	0.988	3.43	1.35	0.998
Pb(II)	2.17	1.35	0.971	8.25	1.64	0.994
Hg(II)	1.07	1.10	0.975	5.15	1.49	0.950

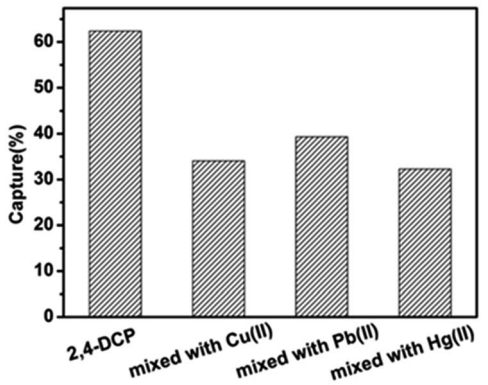

Fig. 6 The adsorption of 2,4-DCP on CD-MS in the presence of different metal ions.

complicated competition behavior occurs in the mixed organic–inorganic solutions. In contrast, all 2,4-DCP adsorptions were depressed when they co-existed with metal ions in the degrees of 37% (Pb(II)), 45% (Cu(II)) and 48% (Hg(II)) (Fig. 6), revealing that the type of metal ions also influences the 2,4-DCP adsorption.

Discussion

Adsorption on pristine mesoporous silica

The surface of MS-ex without high-temperature calcination treatment should be covered with a high-density of silanol groups. Compared with MS-ex, MS-cal has less surface silanols due to its more polymerized silicates frameworks from a calcination treatment at 550 °C for 6 h. The surface of pristine mesoporous silica is dissociated and negatively charged in a neutral environment according to the measured isoelectric point (Fig. 2c). As a π-acceptor compound (*i.e.*, electron-deficient aromatic π-system) due to the presence of two –Cl substituent groups, 2,4-DCP can form n–π electron donor–acceptor (n–π EDA) interaction with oxygen atom on silanol groups.[36,37] Compared with MS-cal, the tripled capture percentage of 2,4-DCP on MS-ex suggests the excellent adsorption performance of CD-MS to 2,4-DCP is partly attributed to the n–π EDA interaction between 2,4-DCP and oxygen atoms on surface silanols since MS-ex and CD-MS are both prepared through template-extraction. Similar capture percentages for different metal ions on MS-cal indicate that the properties of different metal ions have no influence on adsorption behavior. The non-differential improvement of capture percentage on MS-ex further verifies the existence of the same adsorption behavior of different metal ions. The adsorptions of metal ions such as Hg(II), Cu(II) and Pb(II) on pristine mesoporous silica were carried out at pH = 7. Based on the isoelectric point of pristine mesoporous silica (pH = 2, Fig. 2c), the adsorption of metal ions should be attributed to the electrostatic interaction between positively charged metal ions and negatively charged siliceous surface of MS-ex and MS-cal in a neutral environment. The higher adsorption capacity of MS-ex than MS-cal should be attributed to the more negatively charged surface in a neutral environment.

Effect of CD embedding

Compared with pristine mesoporous silica, the mesopore surface of CD-MS is covered with multiple groups of silanol, amides, and aromatic rings (Fig. 2a and b), leading to improved adsorption capacity with different adsorbates. The adsorption performance has also been compared with some recently reported state-of-the-art adsorbent coverings from mesoporous silica modified with different groups (mercapto-, diamine, vinyl-), and organobentonite to polymer (Table S5†). The advantage of CD-MS lies in its excellent adsorption capability for both organic 2,4-DCP and inorganic metal ions. The pronounced improvement of adsorption capacity observed on CD-MS should be attributed to high incorporation content of CD containing amide and aromatic ring groups without the deterioration of pore ordering and accessibility. The hydrophobicity test was further carried out to identify the contribution of hydrophobic interactions due to the presence of aromatic rings in CD. The contact angle increased from 34.65° for MS-ex to 61.59° for CD-MS (Fig. 7), indicating CD-MS is more hydrophobic than pristine mesoporous silica due to CD embedding. However, such kind of hydrophobicity seems incompetent as compared to the significant improvement of adsorption capacity as demonstrated in Fig. 3a since the surface of CD-MS is actually still hydrophilic. In general, hydrophobic interaction refers to the adsorption behavior of aromatic compounds without polar functional groups through a weak van der Waals force. As mentioned above, the presence of two electron-withdrawing –Cl substituents on the aromatic ring should produce an electron-deficient π-system by removing electron density from 2,4-DCP. 2,4-DCP as a π acceptor is adsorbed by pristine mesoporous silica through n–π EDA interaction, which is verified by the increased adsorption of 2,4-DCP on MS-ex compared with that on MS-cal, due to the presence of a higher density of silanol groups on MS-ex. Besides an aromatic ring, CD-MS also contains an amide group, where the O and N atoms should also possibly form n–π a EDA interaction with 2,4-DCP. However, the binding affinity of n–π EDA interactions between 2,4-DCP and dissociated silanol groups is stronger than that caused by hydrophobic interactions since the bonding enthalpies involved in hydrophobic interactions are considered negligible compared with EDA interactions.[38,39] The 2,4-DCP adsorption

on CD-MS is a Langmuir type with homogeneous binding energy. Therefore, it is assumed that a n–π EDA interaction plays a more important role for the improved adsorption due to presence of more N and O atoms. The increased capture percentage of 2,4-DCP with an increasing pH value from 2–8 indicates that the deprotonation of surface silanol has a positive effect on the adsorption capacity (Fig. 3b), which should be attributed to the enhanced n–π EDA interaction between 2,4-DCP and deprotonated atoms with more *n* electrons (O and N). At a pH value below the isotropic point of CD-MS (pH = 5), the hydrogen–π interaction should also be responsible for the high capture percentage. For metal ions, the capture percentages of metal ions all increase with increasing pH values from 2 to 5, which is in accordance with the isoelectric point of CD-MS and attributed to increased electrostatic interactions. The higher adsorption capacity with Hg(II) and Cu(II) should be ascribed to the contribution from a stronger complex tendency of amide groups with Hg(II) through the formation of an inner-sphere surface complex.[40]

Competition between different metal ions

In the tri-metal solution, adsorptions of Cu(II) and Pb(II) show negligible variation, while the adsorption of Hg(II) is depressed compared to the adsorption in the isolate solutions. The total metal ion concentration in the tri-metal solution is higher than that used in the isolate system since the respective concentrations of Hg(II), Cu(II), and Pb(II) in the tri-metal system is set as the same as that in the mono-metal system. In isolate solution, Pb(II) is adsorbed by CD-MS mainly through the electrostatic interaction between positively charged metal ions and negatively dissociated silanols, while Cu(II) and Hg(II) are adsorbed by the extra support from amide groups due to the formation of inner sphere complexes. The preserved adsorption capacity of CD-MS to Cu(II) and Pb(II) in the mixed system indicates there are enough pore volume and adsorption sites to accommodate the increased amount of metal ions. The decreased adsorption of Hg(II) may be attributed to the occupation of the framework surface by hydrated Cu(II) and Pb(II) with large size (0.42 and 0.40 nm of radii),[41] shielding the amide groups from Hg(II) with a smaller hydrated ion size (0.1 nm of radius).[42]

Influence of 2,4-DCP to metal and *vice versa*

The presence of 2,4-DCP does not cause the obvious variation of Hg(II) or Cu(II) adsorption, but it causes a prominent increase of Pb(II) adsorption. The Pb(II) adsorptions are mainly through the electrostatic interaction with a negatively charged surface in the absence of 2,4-DCP. The different effect of 2,4-DCP addition on metal ions can only be ascribed to the complex formation between Pb(II) and the electron-rich chlorine group on 2,4-DCP. In the mixed metal ion–2,4-DCP solution, the 2,4-DCP adsorption always was depressed in the presence of different metal ions. Since the isolate adsorption of 2,4-DCP is attributed to the formation of n–π EDA as demonstrated above, the decreased adsorption in the mixed system should be ascribed to the part shielding of amide groups from 2,4-DCP due to a covering of hydrated metal ions. The more decreased 2,4-DCP adsorption in the presence of Cu(II) or Hg(II) may be ascribed to the strong complexation ability of Cu(II) or Hg(II) with the amide group, which is accordant with the results from the isolate adsorption (Fig. 4a).

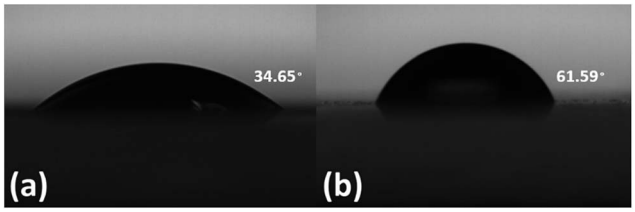

Fig. 7 Images of contact angles of (a) MS-ex and (b) CD-MS.

Conclusion

In this research, we reported a multi-group modified mesoporous silica through the co-condensation of TEOS and silylated CD containing amide groups and aromatic rings. This hybrid material has high adsorption capacity both to organic 2,4-DCP and inorganic Cu(II), Pb(II) and Hg(II). The adsorptions of 2,4-DCP and metal ions follow Langmuir and Freundlich models, respectively, and both of them obey pseudo-second-order kinetics. The efficient 2,4-DCP adsorption is ascribed to the enhanced n–π EDA interaction between 2,4-DCP and an amide group with N and O atoms. Hg(II) and Cu(II) adsorptions have a more prominent improvement than Pb(II) adsorption through forming an inner sphere complex with amide groups on CD. The comprehensive adsorption behavior of each pollutant in a mixed system has been systematically studied on mesoporous silica materials for the first time. In a mixed metal ions system, the Hg(II) adsorption is very depressed due to the shielding of CD NP by other adsorbed metal ions with large hydration radii. In a mixed system of metal ions and 2,4-DCP, the adsorption of 2,4-DCP is ubiquitously depressed due to the presence of metal ions in the order of Cu(II) ≈ Hg(II) > Pb(II), while the Pb(II) adsorption is improved due to its strong complex with Cl group of 2,4-DCP.

Acknowledgements

This work has been supported by the National Nature Science Foundation of China (U1407102, 21322508, 21210004, 21173077 and 21377038), the National Basic Research Program of China (973 Program, 2013CB632403, 2013CB934100, 2012CB224805), the Science and Technology Commission of Shanghai Municipality (14ZR1410700 and 14230710500), the Research Fund for the Doctoral Program of Higher Education (20120074130001), the Program for New Century Excellent Talents in University (NCET) and the Fundamental Research Funds for the Central Universities.

References

1 C. Kresge, M. Leonowicz, W. Roth, J. Vartuli and J. Beck, *Nature*, 1992, **359**, 710–712.

2 J. Hu, X. Wang, L. Liu and L. Wu, *J. Mater. Chem. A*, 2014, **2**, 19771–19777.
3 R. Serna-Guerrero and A. Sayari, *Environ. Sci. Technol.*, 2007, **41**, 4761–4766.
4 A. Walcarius and L. Mercier, *J. Mater. Chem.*, 2010, **20**, 4478–4511.
5 H. Wang, M. Tang, L. Han, J. Cao, Z. Zhang, W. Huang, R. Chen and C. Yu, *J. Mater. Chem. A*, 2014, **2**, 19298–19307.
6 W. Hertl and M. L. Hair, *J. Phys. Chem.*, 1968, **72**(13), 4676–4682.
7 W. Teng, Z. Wu, D. Feng, J. Fan, J. Wang, H. Wei, M. Song and D. Zhao, *Environ. Sci. Technol.*, 2013, **47**, 8633–8641.
8 G. Li, Z. Zhao, J. Liu and G. Jiang, *J. Hazard. Mater.*, 2011, **192**, 277–283.
9 W. Huang, Y. Zhu, J. Tang, X. Yu, X. Wang, D. Li and Y. Zhang, *J. Mater. Chem. A*, 2014, **2**, 8839–8848.
10 I. Emmanuelawati, J. Yang, J. Zhang, H. Zhang, L. Zhou and C. Yu, *Nanoscale*, 2013, **5**, 6173–6180.
11 J. Aguado, J. M. Arsuaga, A. Arencibia, M. Lindo and V. Gascón, *J. Hazard. Mater.*, 2009, **163**, 213–221.
12 M. Meng, X. Meng, Y. Liu, Z. Liu, J. Han, Y. Wang, M. Luo, R. Chen, L. Ni and Y. Yan, *J. Hazard. Mater.*, 2014, **278**, 134–143.
13 Q. Hu, J. J. Li, Z. P. Hao, L. D. Li and S. Z. Qiao, *Chem. Eng. J.*, 2009, **149**(1–3), 281–288.
14 Y. Deng, D. Qi, C. Deng, X. Zhang and D. Zhao, *J. Am. Chem. Soc.*, 2008, **130**, 28–29.
15 X. Yang, C. Chen, J. Li, G. Zhao, X. Ren and X. Wang, *RSC Adv.*, 2012, **2**, 8821–8826.
16 F.-G. Simon and T. Meggyes, *Land Contam. Reclamat.*, 2000, **8**, 103–116.
17 A. Sayari, S. Hamoudi and Y. Yang, *Chem. Mater.*, 2005, **17**(1), 212–216.
18 J. Lei, L. Yang, D. Lu, X. Yan, C. Cheng, Y. Liu, L. Wang and J. Zhang, *Adv. Opt. Mater.*, 2014, **1**(3), 57–63.
19 F. Wang, Z. Xie, H. Zhang, C. Y. Liu and Y. G. Zhang, *Adv. Funct. Mater.*, 2011, **21**, 1027–1031.
20 H. Zhao, K. L. Nagy, J. S. Waples and G. F. Vance, *Environ. Sci. Technol.*, 2000, **34**(22), 4822–4827.
21 M. Anbia and M. Lashgari, *Chem. Eng. J.*, 2009, **150**, 555–560.
22 Q. Qin, K. Liu, D. Fu and H. Gao, *J. Environ. Sci.*, 2012, **24**, 1411–1417.
23 H.-T. Fan, X.-T. Sun, Z.-G. Zhang and W.-X. Li, *J. Chem. Eng. Data*, 2014, **59**(6), 2106–2114.
24 B. Fotoohi and L. Mercier, *Sep. Purif. Technol.*, 2014, **127**, 84–96.
25 A. Shahbazi, H. Younesi and A. Badiei, *Chem. Eng. J.*, 2011, **168**, 505–518.
26 N. Li, Z. Mei and S. Ding, *J. Inclusion Phenom. Macrocyclic Chem.*, 2010, **68**, 123–129.
27 C. Cheng, J. Wang, X. Yang, A. Li and C. Philippe, *J. Hazard. Mater.*, 2014, **264**, 332–341.
28 D. Zhao, J. Feng, Q. Huo, N. Melosh, G. H. Fredrickson, B. F. Chmelka and G. D. Stucky, *Science*, 1998, **279**, 548–552.
29 D. Zhao, P. Yang, N. Melosh, J. Feng, B. F. Chmelka and G. D. Stucky, *Adv. Mater.*, 1998, **10**, 1380–1385.
30 A. Murashkevich, A. Lavitskaya, T. Barannikova and I. Zharskii, *J. Appl. Spectrosc.*, 2008, **75**, 730–734.
31 P. A. Mangrulkar, S. P. Kamble, J. Meshram and S. S. Rayalu, *J. Hazard. Mater.*, 2008, **160**(2), 414–421.
32 D. Karpovich and G. Blanchard, *Langmuir*, 1994, **10**, 3315–3322.
33 Z. Reddad, C. Gerente, Y. Andres and P. Le Cloirec, *Environ. Sci. Technol.*, 2002, **36**, 2067–2073.
34 M. Monier and D. Abdel-Latif, *J. Hazard. Mater.*, 2013, **250**, 122–130.
35 M. Yurdakoç, Y. Seki, S. Karahan and K. Yurdakoç, *J. Colloid Interface Sci.*, 2005, **286**, 440–446.
36 M. Keiluweit and M. Kleber, *Environ. Sci. Technol.*, 2009, **43**, 3421–3429.
37 S. K. Parida, S. Dash, S. Patel and B. Mishra, *Adv. Colloid Interface Sci.*, 2006, **121**, 77–110.
38 A. M. A. Moustafa, K. N. McPhedran, J. Moreira and M. Gamal El-Din, *Environ. Sci. Technol.*, 2014, **48**, 14472–14480.
39 A. Radian and Y. Mishael, *Environ. Sci. Technol.*, 2012, **46**, 6228–6235.
40 H. P. V. Leeuwen and R. M. Town, *Environ. Sci. Technol.*, 2008, **43**, 88–93.
41 B. Tansel, J. Sager, T. Rector, J. Garland, R. F. Strayer, L. Levine, M. Roberts, M. Hummerick and J. Bauer, *Sep. Purif. Technol.*, 2006, **51**, 40–47.
42 D. Grdenić, *Q. Rev., Chem. Soc.*, 1965, **19**, 303–328.

